

# ELECTRONICALLY SCANNED ARRAYS USING MICRO ELECTRO MECHANICAL SWITCH (MEMS) TECHNOLOGY

Mark L. Pugh  
Air Force Research Laboratory  
32 Brooks Road  
Rome, NY 13441-4114

Bill R. Norvell and Robert J. Hancock  
Cae Soft Corporation  
P.O. Box 790  
Caddo Mills, TX 75135

John K. Smith  
Defense Research Projects Agency  
3701 North Fairfax Drive  
Arlington, VA 22203-1714

Sidney W. Theis and James F. Kviatkovsky  
Raytheon Systems Company  
P.O. Box 660246, M/S 8446  
Dallas, TX 75266

## Abstract

The application of Micro Electro Mechanical Switch (MEMS) technology to Electronically Scanned Arrays (ESAs) provides the potential for significantly reducing the volume, weight, cost, and power consumption of antennas for both radar and communications systems. This paper addresses the current and projected status of Radio Frequency (RF) MEMS technology and assesses the potential benefits of MEMS phase shifters for application in ESA antennas. The assessment of potential applications is accomplished by comparing the systems impact of this technology to conventional technologies.

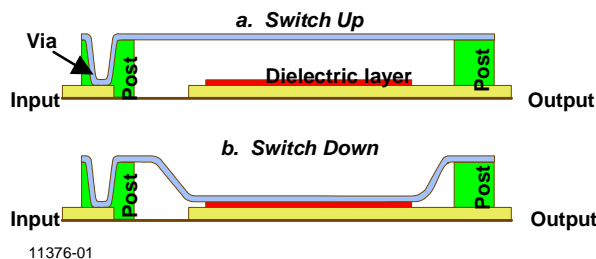
## Introduction

Recent developments in MEMS technology have made possible the design and fabrication of control devices suitable for switching microwave signals. Micromechanical switches were first demonstrated in 1971 [1] as electrostatically actuated cantilever switches used to switch low-frequency electrical signals. Since then, these switches have demonstrated useful performance at microwave frequencies using cantilever [2], rotary [3], and membrane [4] topologies. These switches have shown that moving metal contacts possess low parasitics at microwave frequencies (due to their small size) and are amenable to achieving low on-resistance (resistive switching) or high on-capacitance (capacitive switching). This results in switches with very low loss, electrostatic actuation (no DC current required), and a potential for ultra-linear small-signal operation.

of a DC electrostatic field. A cross-sectional view of a membrane switch element is shown in Figure 1. The upper contact of the switch consists of a 0.3- $\mu\text{m}$  aluminum membrane suspended across polymer posts. Surface micro-machining undercuts the post material from beneath the membrane, releasing it to actuate. The suspended membrane typically resides 4- $\mu\text{m}$  above the substrate surface. On the substrate surface, a bottom contact consists of a 0.7- $\mu\text{m}$  gold or aluminum first metal layer. On top of this first metal layer sits a thin dielectric layer, typically 1,000  $\text{\AA}$  of silicon nitride.

In the unactuated state, the membrane switch exhibits high impedance due to the air gap between the bottom and top metal plates. Application of a DC potential between the upper and lower metal plates causes the thin upper membrane to deflect downwards due to the electrostatic attraction between the plates. When the applied potential exceeds the pull-in voltage of the switch, the membrane deflects into the actuated position. In this state, the top membrane rests directly on the dielectric layer and is capacitively coupled to the bottom plate. This capacitive coupling causes the switch to exhibit low impedance between the two switch contacts. The ratio of the off- to-on impedances of the switch is determined by the on-and-off-capacitance of the switch in the two switching states. Utilizing dielectric coupling prevents problems associated with stiction between the two metal layers as is commonly encountered with dry contact switching.

Micro-mechanical switches can switch RF signals with very low insertion loss, high isolation, high reliability, and very low switching and static power requirements. The signal bandwidth of these switches can approach one decade and designs are practical from a few MHz through 40 GHz. Since the substrate is silicon, the option to integrate control circuitry with the micro mechanical switches is preserved. This technology enables a new way, using established silicon semiconductor processing, to build very thin ESAs for use in radar and communication systems.



11376-01  
**Figure 1. Cross-Sectional Views of Membrane Switch**  
The active element in the micro-mechanical switches is a thin metallic membrane that moves with the application

## MEMS Phase Shifters

MEMS technology can be used to build low-cost, low-loss phase shifters. Switched phase shifters are

implemented by switching in different lengths of line into the RF path to provide incremental phase shifts. Figure 2 illustrates a schematic for a 4-bit phase shifter which uses switches to select combinations of path lengths to provide up to 360 degrees of phase shift with increments of 22.5 degrees.

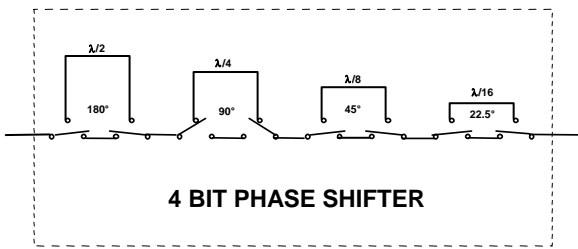


Figure 2. Phase Shifter Schematic

The inherently lower RF path loss and power consumption of the MEMS phase shifter is a key enabler for lower-cost two-dimensional phased array antennas. MEMS devices have demonstrated switching RF signals from 1 GHz to 40 GHz with measured insertion loss of less than 0.2 dB loss per switch up to 40 GHz. The switching speed is approximately 4 microseconds. With this performance it is possible to build low loss digital phase shifters that are fast enough to work in most radar or communication applications. An example of a design layout for a X band (10 GHz) a 4-bit MEMS phase shifter is illustrated in Figure 3. This MEMS phase shifter would measure approximately 6 mm by 9 mm and would have an insertion loss of less than 2 dB.

MEMS are fabricated on silicon wafers which makes them inherently low cost and enables the manufacture of RF phase shifters at 1/40th the cost of GaAs phase shifters. This is achieved at comparable GaAs phase shifter device sizes, with embedded silicon circuit control logic, at lower power consumption, and with the capability to handle RF power signals up to 10 watts. The small size allows hundreds of phase shifters to be built on a single 8 inch silicon wafer for a few dollars cost each.

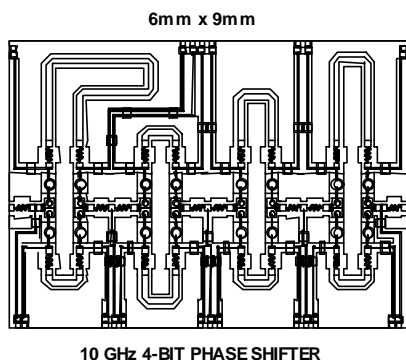


Figure 3. 10 GHz MEMS Phase Shifter

**Electronically Scanned Arrays (ESAs)**

For many applications two-dimensional electronic scan is highly preferred over conventional mechanical gimbal scanning or single dimensional electronic scan because it

does not require any mechanical aperture motion, it enables rapid beam pointing, and it provides flexibility for multi-mission operation. ESAs provide two-dimensional beam steering by controlling the phase of the transmitted and received signal at each radiating element of the aperture. The different type of ESAs can be classified as passive or active depending upon the phase shifter location with respect to amplification.

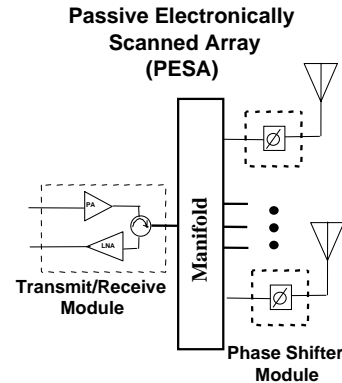


Figure 4. Passive ESA

Passive ESAs use a common transmitter and receiver with phase shifters at each element to electronically steer the antenna beam, as shown in Figure 4. The phase shifters are between the amplifiers and the radiating elements. On transmit the amplifier is referred to as a Power Amplifier (PA) and on receive as a Low Noise Amplifier (LNA). For the passive ESA configuration it is highly desirable for the phase shifters to have low insertion loss since it contributes directly to the RF loss of the aperture and degrades the transmit efficiency and receiver noise figure. It is also desirable for the phase shifters to be light weight and low cost since they account for a significant portion of the total array weight and cost.

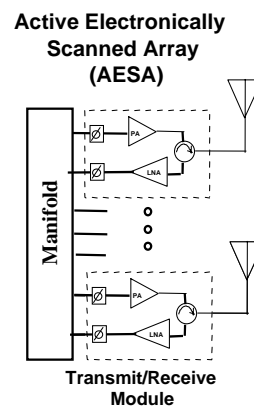


Figure 5. Active ESA

Active ESAs typically place a Transmit/Receive (T/R) module, containing a PA and LNA, behind each radiating element as shown in Figure 5. This minimizes the amount of RF losses that are directly applicable to the system noise figure and transmit efficiency because the phase shifter and manifold are not between the radiating element and the amplification. This provides the lowest phase shifter loss contribution, but can add considerable weight and cost for arrays with many elements.

## MEMS Sub-Array Antennas

The development of an affordable light-weight low-loss MEMS phase shifter makes it possible to consider the design of innovative hybrid antenna concepts which could significantly simplify the design of ESAs, reduce the number of components required, and ultimately reduce the total system cost.

The low-cost manufacturable hybrid approach under consideration utilizes a passive ESA design at the sub-array level with a MEMS phase shifter at each antenna element and a common transmitter Power Amp and receiver LNA for each sub-array. The sub-arrays are then combined in a similar manner as the active ESA with no significant addition to the noise figure by the RF manifold loss after the LNA.

A number of antenna elements can share common GaAs MMICs while achieving good noise figure. Since the phase shifters are built on silicon the resulting array cost can be very low, approaching a few dollars per installed element. An example illustrating how MEMS phase shifters could be used to develop a manufacturable low-cost antenna is shown in Figure 6. The design layout is for a sixteen-element X band sub-array and includes the integration of control circuitry to further reduce complexity and cost.

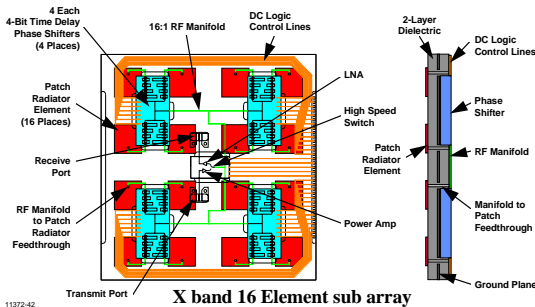


**Figure 6. Design of 16 Element Sub-Array**

### Phase Shifter Comparison

A comparison showing the loss and approximate cost of a 4-bit phase shifters for active and passive ESAs is shown in Table 1. These comparison numbers are based on a combination of measured performance and projected high volume cost of the different phase shifter types.

GaAs FET phase shifters contribute practically no RF loss in active ESA applications because they are not between the antenna element and the amplifier, but the loss is intolerable in a PESA application. The very high loss of the FET also effects the gain requirements of the LNA and thus requiring more LNA power.

The impedance of a PIN diode can be varied with a change in bias control voltage enabling operation as a switch. Digitally switched phase shifters have commonly

used PIN diodes to electronically switch various lengths of transmission line to provide the desired value of phase shift. PIN diode phase shifters can be switched rapidly from one phase state to another, are light-weight and compact in size, have modest insertion loss, and are relatively low cost. The primary disadvantage of PIN diode phase shifters is that they require holding power as well as switching power which can become significant for large arrays.

MEMS devices can be used to micro-mechanically switch various lengths of line to provide a phase shift in a manner similar to Pin diode phase shifters. The MEMS phase shifter is expected to have insertion loss, size, and weight characteristics similar to the PIN diode but cost about one-fourth as much. Additionally, since MEMS phase shifters are electrostatically activated they require essentially no D.C. current which minimizes prime power consumption at the system level.

**Table 1. Phase Shifter Comparison (4-bit)**

Phase Shifter	Power (mW)	Loss(dB)	Cost(\$)
GaAs FET	0	6-10	40
PIN Diode	500-1000	2.0	40
MEMS	0	2.0	10

### ESA Technology Trades

The selection of passive or active ESA system approaches must be weighed against the application and the performance parameter envelope. The development of MEMS phase shifters provides new options for the design of ESA systems that may enable the manufacture of lighter weight radar and communication systems at lower cost.

To support evaluation of MEMS technology for application to ESAs, a system-level trade study was conducted comparing an active ESA with GaAs FET phase shifters and a hybrid ESA concept with passive MEMS sub-arrays. This study did not include PIN Diode phase shifters due to their higher drive power. This trade is similar to a study performed for a Space-Based Radar application [5].

The study concentrated on the aperture power requirements using parametric values of the radiated power and LNA power requirements per element. This trade was done for a point design of the RF losses and manifold loss model that is discussed below. The manifold loss model is for X-Band and thus limits the validity of this study to that frequency.

To maintain a constant performance the radiated power ( $P_r$ ) was increased by the one-way RF loss. This compensated for the receiver noise figure differences due to the different RF losses that occur with the different implementations. Assuming the transmit and receive RF losses are the same, the amount of power generated by the Power Amps ( $P_{pa}$ ) is the radiated power ( $P_r$ ) increased once again by the one-way RF loss.

To facilitate interpretation of this trade the concept of normalized radiated power ( $P_n$ ) is introduced. This is the amount of radiated power that must be provided to obtain the SNR performance when no RF losses are considered. This leads to the following relationships for maintaining equal performance:

$$\begin{aligned} P_r [\text{dB}] &= P_n [\text{dB}] + L_{rf} [\text{dB}] \\ P_{pa} [\text{dB}] &= P_n [\text{dB}] + 2L_{rf} [\text{dB}] \end{aligned} \quad (1)$$

The RF losses are shown in Table 2 for the AESA and Table 3 for the hybrid PESA. The common losses associated with the circulator and the element are nominal values from the author's ESA experience.

**Table 2. AESA RF Losses**

Parameter	Value
Circulator Loss (1-Way)	0.5 dB
Element Loss (1-Way)	0.5 dB
$L_{rf}$ - One Way RF Loss	1.0 dB
$L_{rf2}$ - Two Way RF Loss	2.0 dB

**Table 3. PESA RF Losses**

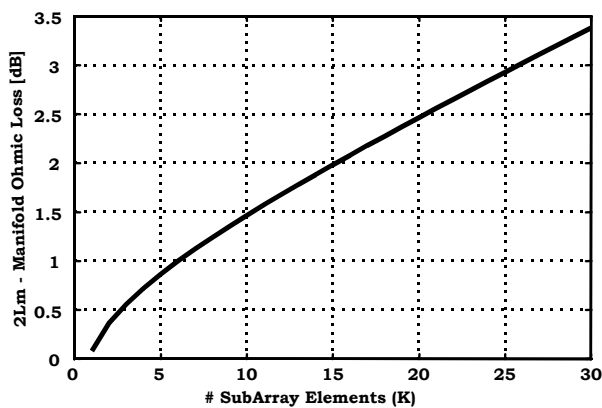
Parameter	Value
Circulator Loss (1-Way)	0.5 dB
Element Loss (1-Way)	0.5 dB
MEMS Phase Shifter (1-Way)	2.0 dB
$L_m$ - Manifold Loss (1-Way)	Function of # elements In Sub-Array (K)
$L_{rf}$ - One Way RF Loss	3.0 dB + $L_m$
$L_{rf2}$ - Two Way RF Loss	6.0 dB + $2L_m$

In the hybrid PESA implementation, the manifold losses varied with the number of elements in a sub-array (K). The RF loss in the manifold ( $L_m$ ) is model as:

$$L_m = (\ln(K) / \ln(2) * 0.1) + (K/2 * 0.08) \quad (2)$$

Where the first term is for the power splitters and the second term is for the line length loss when the modules are in a linear configuration. The two-way RF loss ( $2L_m$ ) due to the manifold is shown in Figure 7.

Nominal stripline loss is approximately 0.2 dB/inch. For half wavelength spacing, this corresponds to approximately 0.08 dB/radiator. For purposes of this trade the power splitters are assumed to be 0.1 dB per power splitting level. As an example, an 8 way RF circuit then has three splitters for 0.3 dB loss plus 0.32 dB of transmission line loss for a total of 0.62 dB making the



two way loss equal to 1.24 dB.

**Figure 7: Manifold RF Loss (2-way) –  $2L_m$**

The amount of prime power required power required by the power amps ( $PWR_{pa}$ ) depends on the amplifier efficiency:

$$PWR_{PA} = P_{PA} / \text{Eff}_{PA} \quad (3)$$

where  $PWR_{PA}$  is the power generated by all the power amplifiers and  $\text{Eff}_{PA}$  is their efficiency.

The model used for power amplifier efficiency is shown in Figure 8. The model shows high efficiencies at low powers and decreasing efficiencies as the power generated by the power amplifier increases.

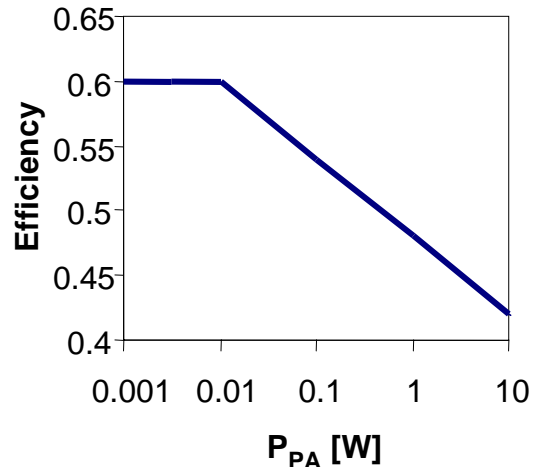
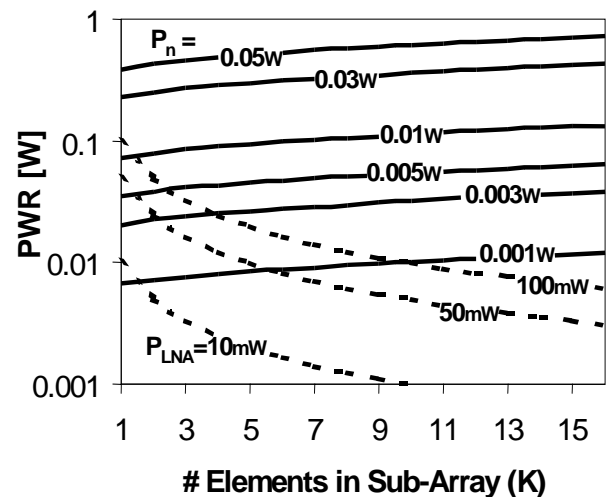


**Figure 8: Power Amplifier Efficiency Model**

The LNA power required is a function of the dynamic range, third order intercept, and the gain required. For this study we used parametric values of 10, 50 and 100 mW per LNA.

The hybrid PESA power trade process determines the number of elements that will be sub-arrayed to minimize the total power of the array. There are opposing power requirement trends as a function of the number of elements in the sub-array (K). As K increases the manifold losses increase and more power is required by the power amplifiers, however, there are fewer LNAs and thus the LNA power per element is inversely proportional to K. These two relationships are shown in Figure 9 as a function of the number of elements in the sub-array (K). The solid lines represent the PA power required power per element ( $PWR_{pa}$ ) for different values



of  $P_n$  and the dashed lines represent the LNA power required ( $P_{WRlna}$ ) per element for different LNA device powers.

**Figure 9: Required PA and LNA power as a function of sub-array size**

To complete the power trade study a constant control power of 5 mW was used for both the AESA and PESA phase shifters. The total array power required ( $P_{tot}$ ) is the summation of that required for the power amplifier, the LNA and the control function.

As an example, for  $P_n$  equal to 0.003W,  $P_{tot}$  was plotted against  $K$  for LNA powers of 10, 50, and 100mW in Figure 10. The minimum total power occurs at different values of  $K$ . The most notable PESA power reductions occur with the larger values of LNA Power.

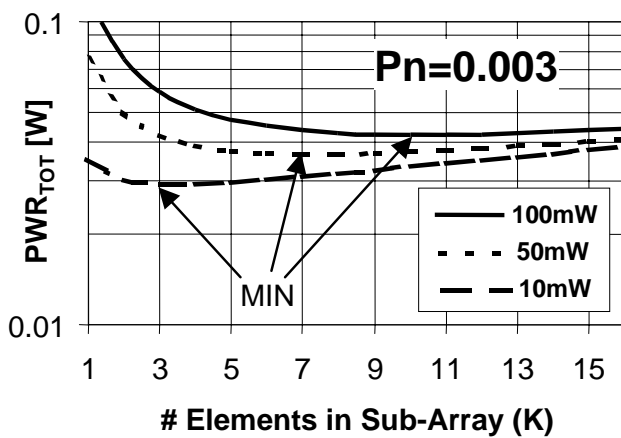


**Figure 10. Total Power Required For  $P_n=0.003$**

The PESA minimum total power values for each of the values of  $P_n$  used in Figure 9 were computed with the three LNA powers. These were plotted against  $P_n$  along with the AESA total powers in Figures 11 and 12. For clarity Figure 11 has LNA powers of 10 and 100mW and Figure 12 has LNA power of 50mW. The crossover values of  $P_n$  where the designs have equal total power is noted. These values were used to develop a figure that provides insight into the system parameters and array sizes that favor either the hybrid PESA or the AESA

**Figure 11. Minimum Total PESA and Total AESA power required values as a Function of  $P_n$ . (LNA powers of 10 & 100 mW)**

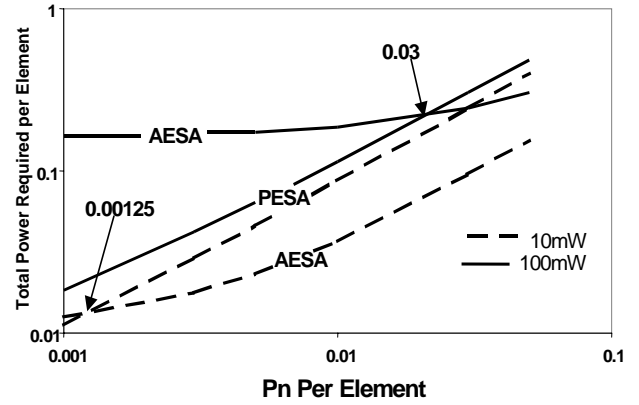
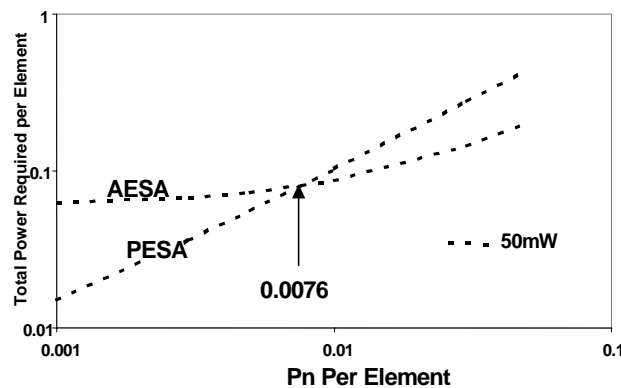


**Figure 12. Minimum Total PESA and Total AESA power required values as a Function of  $P_n$ . (LNA powers of 50 mW)**

design implementations. To do this the results shown in Figures 11 & 12 were extended to an entire aperture by taking the AESA/PESA equal element power numbers as a function of  $P_n$  at the element and multiplying them by the number of elements in postulated arrays. The results are shown in Figure 13.

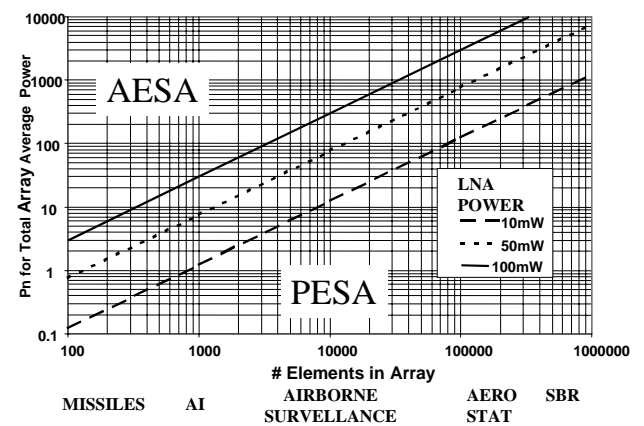


**Figure 13. AESA- PESA Trade Space Summary for Different Array Power and Sizes for Three LNA Powers and Losses shown in Tables 3 & 4.**

**Conclusions**

For a hypothesized system to counter a given threat one of the first things that is know is the power aperture product required. By entering the figure along the x-axis with the size of the aperture and along the y-axis with the total array normalized radiated power the user can plot the operating point on the graph. Depending upon the LNA power required to provide the necessary gain and third order intercept, the user can determine the operating point with respect to the LNA power line. The further above it is the more the design favors the AESA and the further below it is the more the design favors the Hybrid PESA.

The reader is advised that the numbers and equations that are used in this paper are rough estimates that generally are more optimistic than actual hardware results. The relationship between parameters is also more complex than indicated by the trade. These liberties were taken to simplify the presentation. The results do not negate the trends but may modify the absolute values of the results.

**Summary**

MEMS applied to Electronically Scanned Arrays offer a way to greatly reduce the cost and weight and power consumption for systems that have low transmit per element and high LNA power requirements. This is usually the case with large apertures. The methodology shown in this paper can be used as the trade space is varied to consider different RF Loss, PA and LNA parameters. RF MEMS are just now becoming practical for these applications and performance increases for RF MEMS should be expected as the technology matures.

### References

- [1] K.E. Peterson, 'Micromechanical Membrane Switches on Silicon', IBM Journal of Research and Development, vol. 23, no. 4, pp. 376-385, July 1979.
- [2] J.J. Yao and M.F. Chang, 'A Surface Micromachined Miniature Switch for Telecommunications Applications with Signal Frequencies from DC up to 4 GHz', Proceedings of Transducers '95 Conference, pp. 384-387, June 1995.
- [3] L.E. Larson, R.H. Hackett, M.A. Melendes, and R.F. Lohr, 'Micromachined Microwave Actuator (MIMAC) Technology - A New Tuning Approach for Microwave Integrated Circuits', Proceedings of the IEEE Microwave Theory Technical Symposium, pp. 27-30, June 1991.
- [4] C. Goldsmith, T.H. Lin, B. Powers, W.R. Wu, B. Norvell, 'Micromechanical Membrane Switches for Microwave Applications', Proceedings of the IEEE Microwave Theory Technical. Symposium, pp. 91-94, May 1995.
- [5] B. Norvell, R. Hancock, J. Smith, M. Pugh, S. Theis and J. Kviatkofsky, 'Micro Electro Mechanical Switch (MEMS) Technology Applied to Electronically Scanned Arrays for Space Based Radar', Proceedings of the IEEE Aerospace Conference, Snowmass, CO, March 1999

